DYNAMIC RESPONSE ANALYSES FOR SHAKE TABLE TESTS OF FULL-SCALED REINFORCED CONCRETE BRIDGE COLUMN MODEL

J. Sakai[1] and S. Unjoh[2]

[1] *Senior Researcher, Center for Advanced Engineering Structural Assessment and Research , Public Works Research Institute, Tsukuba. Japan, sakai55@pwri.go.jp*

[2] *Chief Researcher, Center for Advanced Engineering Structural Assessment and Research , Public Works Research Institute, Tsukuba. Japan, unjoh@pwri.go.jp*

ABSTRACT :

A series of dynamic response analyses for shake table tests of a full-scaled reinforced concrete bridge column model was conducted, and the effect of viscous damping properties, structural modeling on the accuracy of the analyses was investigated. The specimen analyzed is the one that is designed to be failed in flexure at the bottom of the column, and was tested on the E-Defense in 2007. A test setup used is consisted of two girders supported by bearings on the tested specimen and the end-supports. Two analytical models are considered, and the results are compared; one is a simple single-column model and the other is an entire system model including the idealization of the girders and the bearings. The nonlinear behavior of the reinforced concrete column is idealized with fiber elements for both the models. The analyses underscored that it is important to idealize the bearing supports adequately. Almost zero damping provides good agreement with the test results.

KEYWORDS: reinforced concrete bridge column, shake table test, full scale, fiber element, dynamic response analysis

1. INTRODUCTION

A research program on bridge structures using the E-Defense has been conducted since 2005 (Kawashima et al. 2008), which includes a series of shake table tests for full-scaled reinforced concrete bridge column models. The test project are expected to provide valuable information on the failure mechanism of reinforced concrete bridge columns that were severely damaged during the big event as well as on the effect of specimen size on the evaluation of the seismic performance and dynamic failure mechanism, and on the development of advanced analytical models. One of the shake table tests had been conducted in 2007 for a full-scaled bridge column specimen modeling a column that suffered severe flexural damage at the bottom of the column during the 1995 Hyogo-ken Nanbu earthquake.

To evaluate the accuracy of the analytical models and clarify the issues that to be studied for development of advanced models, a series of dynamic analyses was conducted. The effects of viscous damping properties, structural modeling on the accuracy of the analyses was investigated.

2. OVERVIEW OF SHAKE TABLE TEST (Kawashima et al. 2008)

2.1. Test setup and specimen

Figure 1 shows the test setup and the specimen. Two girders, which steel blocks as weights are fixed to, are supported by fixed bearings on the top of the specimen and a longitudinal-movable/ transverse-fixed bearing at each end. Two sliding bearing are placed on each side of the fixed bearing on the specimen to prevent overturning of the girders. Due to this setup, the inertia force of the girder-block assembly is applied to the top of the specimen (7.5 m from the bottom of the column) in the longitudinal direction, and to the center of the gravity of the girder-block assembly (9.14 m from the bottom) in the transverse direction. The inertia mass of each girder-block assembly is 145 ton. Since all the inertia force is applied to the specimen due to the boundary condition, the inertia mass of the girder-block assembly in the longitudinal direction is 289 ton. In the

transverse direction, on the other hand, not only the specimen but also the end supports carry the inertia force. Thus, the inertia mass of the girder-block assembly in the transverse direction is 199 ton.

The diameter of the column is 1.8 m, and the height of the column is 7.5 m. 80 of SD345, 29-mm-diameter deformed bars are arranged as the longitudinal reinforcement. The longitudinal reinforcement ratio ρ_l is 2.02%. As a transverse reinforcement, SD345, 13-mm-diameter deformed bars are provided. The pitch of the transverse hoops is set at 300 mm excluding the both ends of the column. In the region of about 1 m from the bottom and the top of the column, the outer transverse reinforcement is arranged at 150-mm-pitch. The transverse reinforcement ratio ρ_s is 0.42% around the bottom. The transverse reinforcement is anchored with lap splices, and the anchorage length is 300 mm.

The design strength of the concrete f_{c0} is set to be 27 N/mm^2. The design yield strength f_{sy} of SD345 bars are 345 N/mm^2. Table 1 shows the material properties obtained from the material tests.

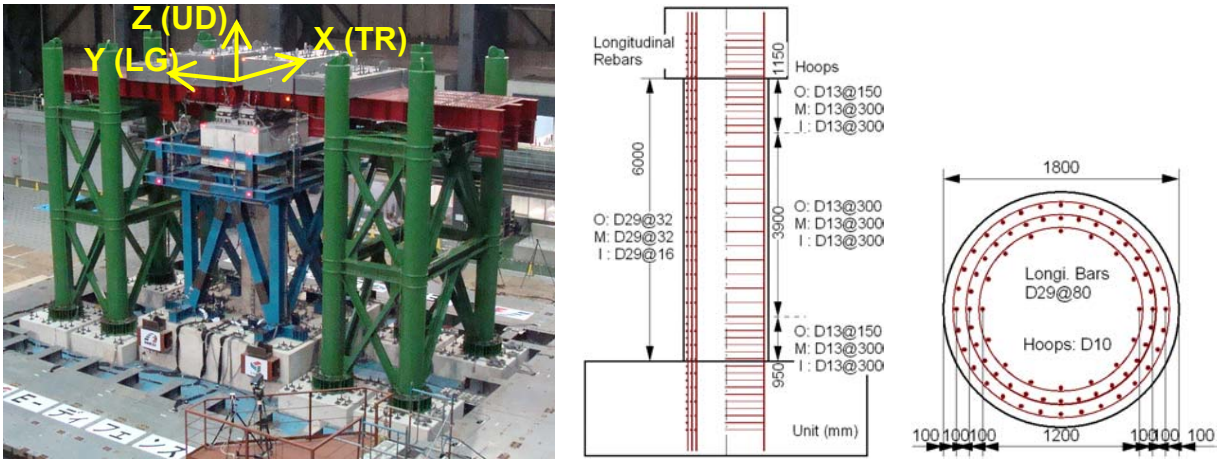

(a) Test setup (b) Flexural failure specimen (c) Cross section

Figure 1 Test setup and full-scaled bridge column specimen

Table 1 Material Properties

(a) Concrete

	f_{c0} (N/mm^2)	E_c (kN/mm^2)
ϕ100 X 200 Cylinders	34.1	25.9
ϕ150 X 300 Cylinders	32.6	26.1
ϕ100 Cylinders from 1m^3 Block	33.0	25.1

(b) Reinforcing steel

	f_{sy} (N/mm^2)	E_s (kN/mm^2)
Longitudinal bars	366.0	193.0
Hoops (Outer)	377.7	205.7
Hoops (Middle)	376.3	197.0
Hoops (Inner)	381.7	188.7

The specimens were tested under three dimensional ground motions. Ground accelerations measured at JR Takatori station during the 1995 Kobe earthquake (Nakamura, 1995) were selected for this study and the NS, EW and UD components were inputted in the longitudinal, transverse, and vertical directions, respectively. Taking account of the soil-structure-interaction effect, the amplitude of the motions was scaled by 80%, and this motions are named the 100% experimental JR Takatori ground motion (E-Takatori). The tests had two phases; one is for dynamic response in elastic range, and the other is for that in nonlinear range. 10%, 20%, 30% of the E-Takatori ground motions were used for the elastic level tests. For the nonlinear level tests, 100% of the E-Takatori ground motions were inputted to the table. A test using the 100% E-Takatori ground motions were conducted twice.

2.2. Dynamic response of specimen

No crack was observed after the elastic level test. The fundamental natural periods prior to the nonlinear level

tests were 0.5 seconds and 0.6 seconds in the longitudinal and transverse directions, respectively.

As shown in Figures 10 to 13, the maximum response displacements at the top of the specimen (7.5 m from the bottom of the column) were 0.173 m and 0.134 m in the longitudinal and transverse directions, respectively, and 0.195 m as a distance from the origin, which was twice of the computed ultimate displacement. Figure 2 (a) show the damage after the first nonlinear level test. Spalling of cover concrete and minor buckling of longitudinal reinforcement were observed. Residual displacements were 0.02 m in both the directions.

Figure 2 (b) shows the final failure mode after the second nonlinear test. During the second test, the maximum response displacements increased up to 0.314 m as a distance from the origin. Flexural damage extended due to this lateral displacement. Residual displacements in the longitudinal and transverse directions decreased during the second test.

(a) After first nonlinear test (b) After second nonlinear test

Figure 2 Flexural damage at Yp (W) face

3. ANALYTICAL IDEALIZATION

The specimen is idealized as a three-dimensional discrete model as shown in Figure 3. Two analytical models are considered; one is a simple single-column model and the other is an entire system model including the idealization of the girders, steel blocks and bearings. The same idealization for the column was used for both models. The nonlinear hysteretic behavior of the column is idealized with fiber elements. The element length is set to be 0.9 m, a half of the diameter of the cross section, which is equivalent to the plastic hinge length specified in the JRA specifications (2002). Concrete section was divided into 800 fibers. Linear beam elements with uncracked stiffness properties are used to model the footing and the top slab of the column. P-Δ effect was included in the analysis.

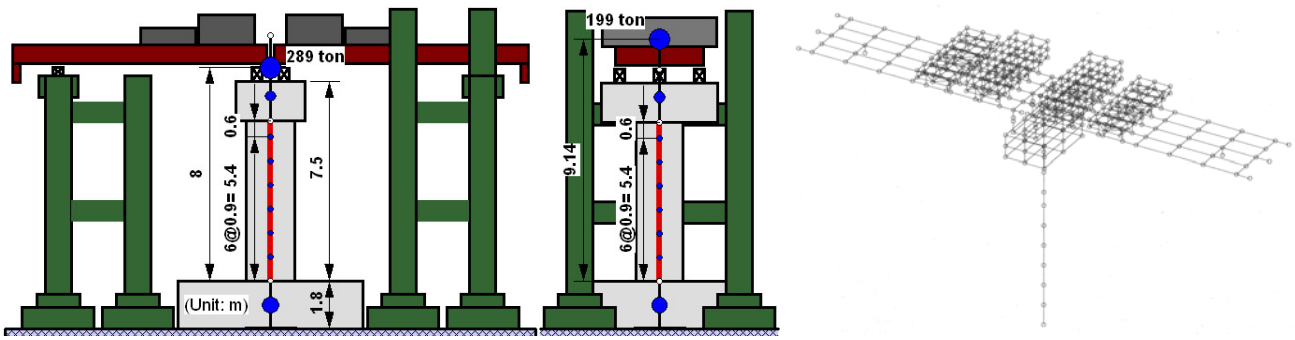

(a) Single-column model (b) Entire system model

Figure 3 Test setup and full-scaled bridge column specimen

To evaluate the confinement effect of core concrete, the model proposed by Hoshikuma et al. (1997) was used. The envelope curve is also idealized with the model proposed by Hoshikuma et al. In the descending branch of the stress-strain relation, the stress becomes constant when the stress decreases to 20% of the peak stress as shown in Figure 4. In the descending branch of the stress-strain relation of cover concrete, the stress reaches

zero at the concrete strain of 0.005.

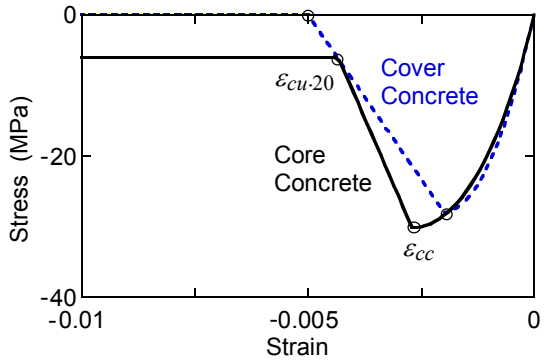

Figure 4 Envelope curves of stress-strain relation of concrete

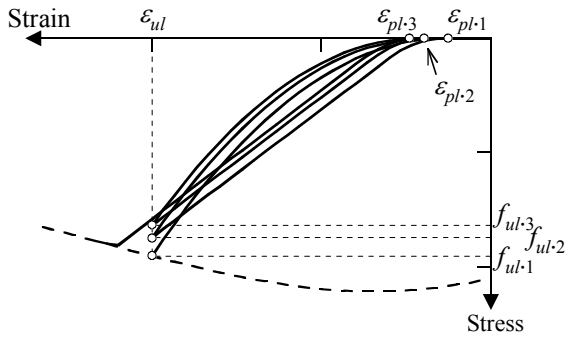

Figure 5 Unloading and reloading paths of concrete

Figure 5 shows the unloading and reloading paths of concrete, which are idealized by the model proposed by Sakai and Kawashima (2006). An unloading path from the envelope curve and reloading from zero stress are idealized as

$$f_c = f_{ul\cdot 1}\left(\frac{\varepsilon_c - \varepsilon_{pl\cdot 1}}{\varepsilon_{ul} - \varepsilon_{pl\cdot 1}}\right)^2 ; \quad f_c = \begin{cases} 2.5 f_{ul\cdot n}\left(\dfrac{\varepsilon_c - \varepsilon_{pl\cdot n}}{\varepsilon_{ul} - \varepsilon_{pl\cdot n}}\right)^2 & \left(0 \le \dfrac{\varepsilon_c - \varepsilon_{pl\cdot n}}{\varepsilon_{ul} - \varepsilon_{pl\cdot n}} < 0.2\right) \\ E_{c\cdot rl}(\varepsilon_c - \varepsilon_{ul}) + f_{ul\cdot n+1} & \left(0.2 \le \dfrac{\varepsilon_c - \varepsilon_{pl\cdot n}}{\varepsilon_{ul} - \varepsilon_{pl\cdot n}} \le \dfrac{\varepsilon_{re} - \varepsilon_{pl\cdot n}}{\varepsilon_{ul} - \varepsilon_{pl\cdot n}}\right) \end{cases} \quad (3.1); (3.2)$$

where

$$\varepsilon_{pl\cdot 1} = \begin{cases} 0 & (0 \le \varepsilon_{ul} \le 0.001) \\ 0.43(\varepsilon_{ul} - 0.001) & (0.001 < \varepsilon_{ul} < 0.0035) \\ 0.94(\varepsilon_{ul} - 0.00235) & (\varepsilon_{ul} \ge 0.0035) \end{cases} \quad (3.3)$$

$f_{ul\cdot 1}$ and ε_{ul} are the unloading stress and strain on the envelope curve, $f_{ul\cdot n}$ is the stress at unloading point after nth unloading/reloading, $\varepsilon_{pl\cdot n}$ is the plastic strain after nth unloading/reloading, ε_{re} is the strain at the point where reloading path intersects the envelope curve, and $E_{c\cdot rl}$ is the reloading modulus.

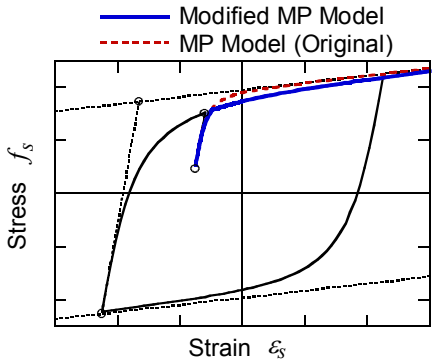

Figure 6 Modified Menegotto-Pinto model

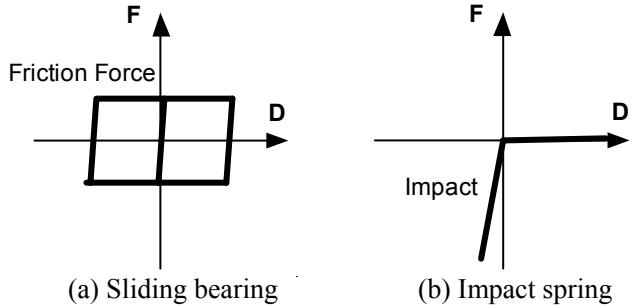

(a) Sliding bearing (b) Impact spring

Figure 7 Idealization of bearings

Modified Menegotto-Pinto model, shown in Figure 6, proposed by Sakai and Kawashima (2003) was used to idealize the stress vs. strain relation as:

$$f_s = \begin{cases} f_{s1} & (f_{s1} \le f_{sp}) \\ f_{sp} & (f_{s1} > f_{sp}) \end{cases} \quad \text{(For tensile loading)} \tag{3.4}$$

$$f_s = \begin{cases} f_{s1} & (f_{s1} \le f_{sp}) \\ f_{sp} & (f_{s1} > f_{sp}) \end{cases} \quad \text{(For compressive loading)} \tag{3.5}$$

where

$$f_{s1} = \tilde{f}(f_0 - f_r) + f_r \,; \quad f_{sp} = \tilde{f}_p (f_{0p} - f_{rp}) + f_{rp} \tag{3.6); (3.7}$$

and where

$$\tilde{f} = \frac{f_s - f_r}{f_0 - f_r} \,; \quad \tilde{f}_p = R_s \tilde{\varepsilon}_p + \frac{(1 - R_s)\tilde{\varepsilon}_p}{\left(1 + \tilde{\varepsilon}_p^{\,R_{bp}}\right)^{1/R_{bp}}} \,; \quad \tilde{\varepsilon}_p = \frac{\varepsilon_s - \varepsilon_{rp}}{\varepsilon_{0p} - \varepsilon_{rp}} \tag{3.8); (3.9); (3.10}$$

R_s is the strain hardening ratio, R_{bp} is the Bauschinger effect coefficient after partial unloading, f_r is the steel stress at reversal point, f_{rp} is the steel stress at reversal point after partial unloading, f_0 is the steel stress at intersection of two asymptotes, f_{0p} is the steel stress at intersection of asymptotes after partial unloading, ε_{rp} is the steel strain at reversal point after partial unloading, ε_{0p} is the steel strain at intersection of asymptotes after partial unloading.

Because the effect of buckling of longitudinal reinforcement is not considered in the analysis, this analysis has an ability to predict the behavior before the occurrence of rebar buckling.

For the entire system model, the girders and steel blocks are idealized with linear beam elements. Figure 7 shows the idealization of the bearings. Fixed bearings, which were placed on the top of the specimen, are idealized with elastic spring elements. Longitudinal-movable/transverse-fixed bearings at the end-supports are idealized by nonlinear spring elements with friction type hysteretic behavior and linear spring elements, respectively. Because the friction force of the movable bearings was not measured in the shake table tests, the friction coefficient was varied from 0% to 30%. Dependency of the friction coefficient on the vertical load and the velocity is not included in the analysis. Impact springs are used to idealize the vertical behavior of the sliding bearing placed on the sides of the fixed bearings on the specimen because rotational behavior of the girders around the longitudinal axis due to the transverse response of the column resulted in separation and contact at the surface of the sliding bearings. The friction force of the sliding bearings on the specimen is not considered in the analysis for simplicity sake because the effect of the varying axial force on the friction force is not able to be idealized by simple spring models.

For the single-column model, rigid beam elements are used for the elements from the top of the column to the center of gravity of the steel blocks-girders assembly. The concentrated mass is set at 7.5 m and 9.14 m from the bottom of the column in the longitudinal and transverse directions, respectively, to idealize the inertia mass of the girder-block assembly (= 289 ton and 199 ton in the longitudinal and transverse directions).

Rayleigh damping was used to idealize viscous damping properties as shown in Figure 8. 2% and 0.1% of the damping ratios were considered, and two fundamental frequencies were set to be 2 Hz and 50 Hz. The case using 0.1% for the damping ratio intended to represent no viscous damping, but small viscous damping was considered for numerical stability.

As input ground motions in the analyses, 100% E-Takatori ground motions, which was the command signal, and accelerations measured at the top of the footing are used. Figure 9 compares the acceleration response spectra between those two motions.

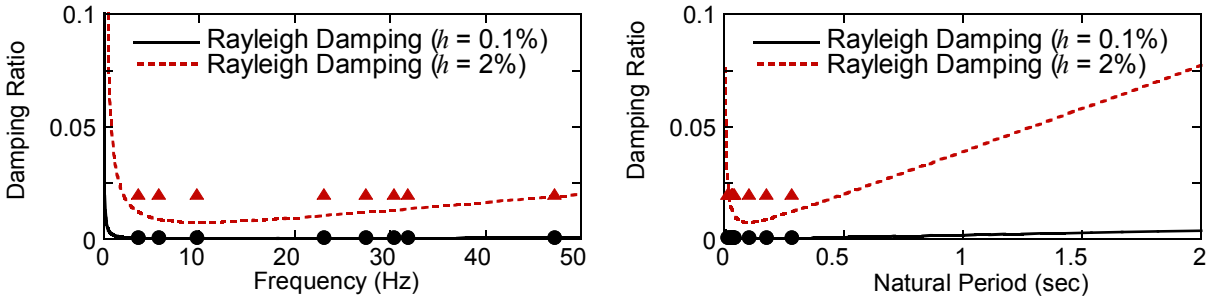

(a) Damping ratio vs. frequency relation (b) Damping ratio vs. natural period relation

Figure 8 Rayleigh damping

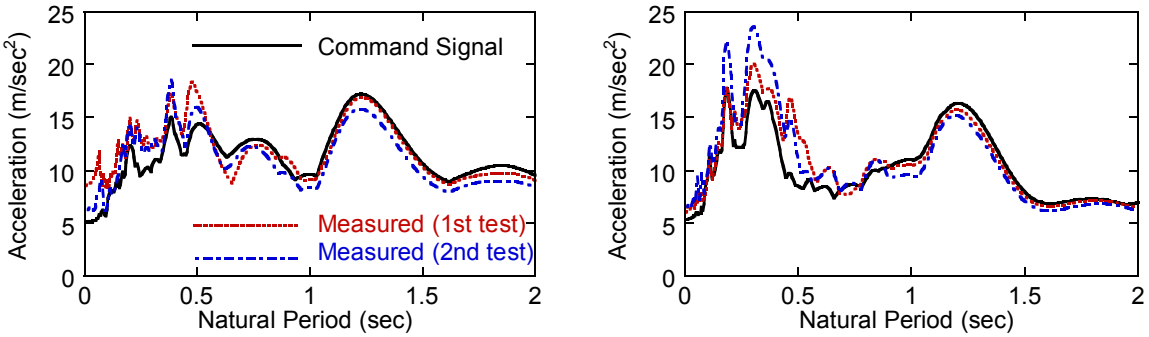

(a) Longitudinal direction (b) Transverse direction

Figure 9 Acceleration response spectra

4. ACCURACY OF FIBER ANALYSIS

Figure 10 shows the effect of the input ground motions for the entire system model. A damping ratio of 0.1% and a friction coefficient of 20% are considered here. When the command signals are used, the analysis predicts 150% larger response displacement in the longitudinal direction while using the measured acceleration results in sufficient accuracy.

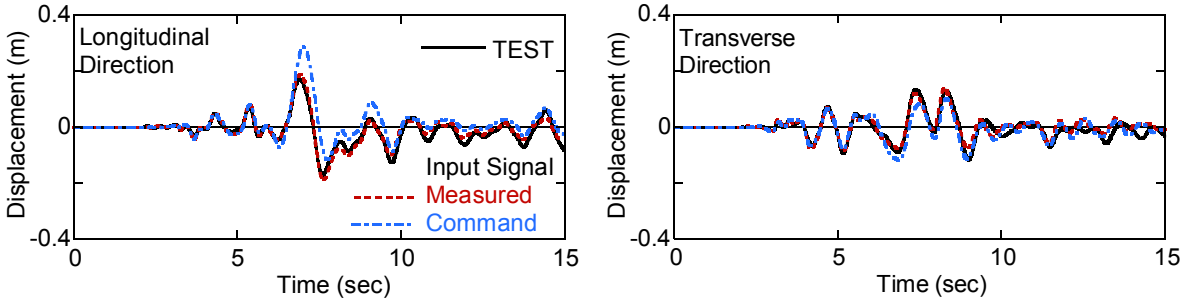

Figure 10 Effect of input ground motions

Figure 11 shows the accuracy of the analysis using the simple single-column model when the damping ratio and the friction coefficient are fixed to 0.1% and 20%, respectively, and the measured accelerations are used here. Both models provide good prediction in the response in the transverse direction while the single-column model provides larger response displacement in the longitudinal direction, which implies the importance of the idealization of the movable bearing on the end-supports.

Figure 12 shows the effect of the idealization of friction force of the movable bearings at the end-supports for the entire system model. A damping ratio of 0.1% is assumed and the measured accelerations are used here.

Smaller friction coefficient provides larger response displacement. Among the values considered here, a friction coefficient of 20% provides the best prediction.

When a damping ratio of 2% is assumed, the analysis predicts 14% smaller response displacement than the actual response during the test. When almost zero damping (the damping ratio = 0.1 %) is assumed, the analysis predicts 3% larger response displacement, resulting in better accuracy as shown in Figure 13.

According to these results, if the measured acceleration is used as input ground motions, a friction coefficient of 20% is used, a damping ratio of 0.1% is assumed, and the entire system model is used, the analysis provides good agreement with the test results.

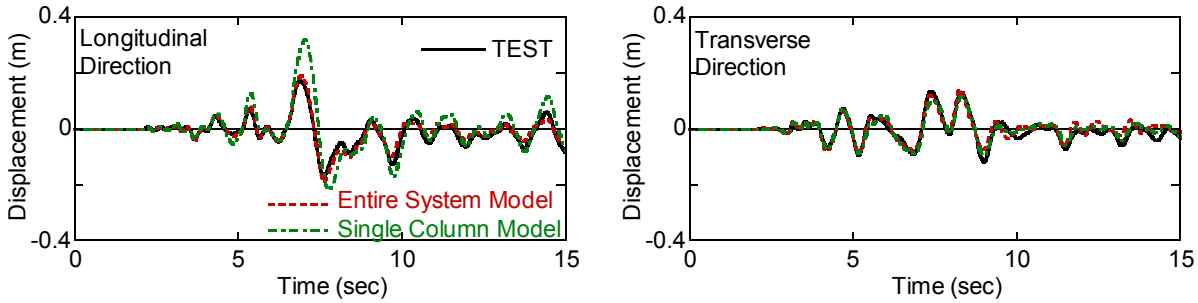

Figure 11 Accuracy of single-column-model

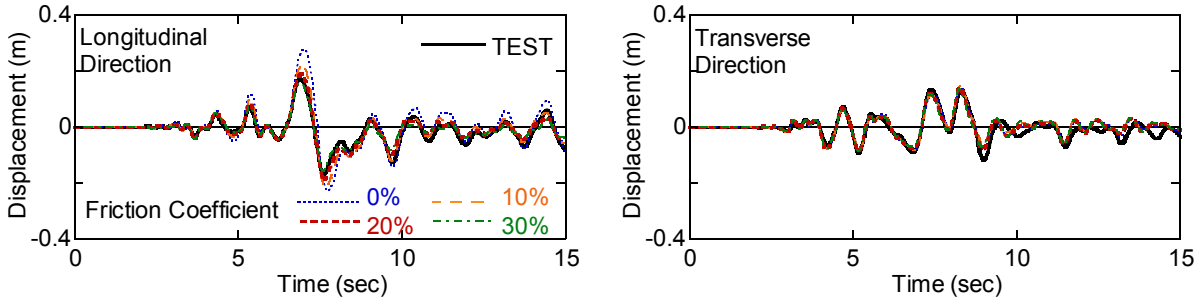

Figure 12 Effect of friction coefficient of movable bearings at end-supports

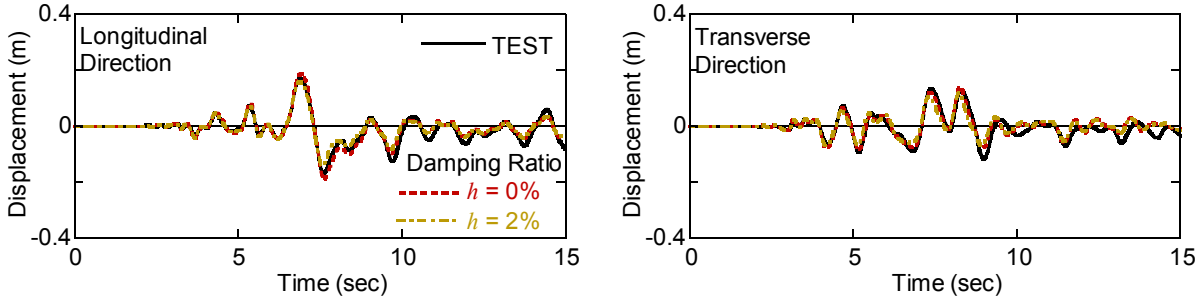

Figure 13 Effect of damping assumption

As described above, the model used here does not have an ability to predict post-peak behavior. However, to investigate how the current model predicts the post-peak behavior, the analysis was conducted for the second nonlinear test under the E-Takatori 100% excitation. The measured accelerations, a friction force of 20%, a damping ratio of 0.1%, and the entire system model are used.

Figure 14 shows the accuracy of the analysis for the second nonlinear test. The analysis predicts larger residual displacement as well as larger peak response displacement. This may be because of flexural strength deterioration in the analysis, which is resulted from small reaction force assumed in the post-peak modeling of

concrete. No consideration of rebar buckling might have relatively smaller effect. It is necessary to develop an analytical model that can predict the post failure response and behavior until collapse.

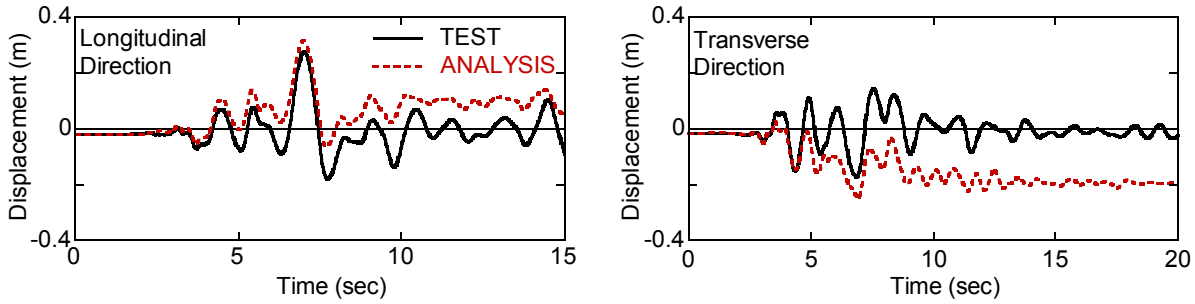

Figure 14 Accuracy of analysis for 2nd 100% E-Takatori ground motions

5. CONCLUSIONS

A series of dynamic analyses was conducted to evaluate the accuracy of the analytical models and clarify the issues that to be studied for development of advanced models. Fiber elements are used to idealize the nonlinear behavior of a reinforced concrete bridge column. The effects of viscous damping properties, structural modeling on the accuracy of the analyses was investigated. Below are the conclusions determined from the study:

1. It is significant to idealize the behavior of the bearings properly to predict the response with sufficient accuracy. For the test setup used, the modeling of the movable bearing at the end-supports has significant effects on the accuracy of the dynamic analyses.
2. Assuming almost zero viscous damping provides better agreement with the test results.
3. The current analytical modeling has an ability to predict the response until the rebar buckling occurs. It is necessary to develop analytical models to predict post-damage behavior.

ACKNOWLEDGEMENTS

The authors extended their appreciation to the members of the executive committee for the E-Defense research program of bridge structures (Chair: Prof. Kazuhiko Kawashima) for their valuable advices.

REFERENCES

Hoshikuma, J., Kawashima, K., Nagaya, K. and Taylor, A. W. (1997) Stress-strain model for confined reinforced concrete in bridge piers. *J. Struct. Engrg*, ASCE, **123: 5**, 624-633.

Japan Road Association (JRA) (2002). Part V Seismic design, Design specifications of highway bridges. Maruzen, Tokyo, Japan.

Kawashima, K., Sasaki, T., Kajiwara, K. Ukon,U. Unjoh, S., Sakai, J., Kosa, K., Takahashi, Y. and Yabe, M. (2008). Seismic performance of a flexural failure type RC bridge column based on E-Defense excitation. *Proc. 40th Panel on Wind and Seismic Effect*, UJNR, Gaithersburg, MD, USA.

Nakamura, Y. (1995). Waveform and its analysis of the 1995 Hyogo-ken Nanbu earthquake. *JR Earthquake Information* **23c**, Railway Technical Research Institute, Japan.

Sakai, J. and Kawashima, K. (2006) Unloading and reloading stress-strain model for confined concrete. *J. Struct. Engrg.*, ASCE, **132:1**, 112-122.

Sakai, J. and Kawashima, K. (2003) Modification of the Giuffre, Menegotto and Pinto model for unloading and reloading paths with small strain variations. *J. Struc. Mech. Earthq. Engrg.*, JSCE, **738/I-64**, 159-169.